HHS Public Access

Author manuscript

Biochem Biophys Res Commun. Author manuscript; available in PMC 2020 August 13.

Published in final edited form as:

Biochem Biophys Res Commun. 2019 August 13; 516(1): 313–319. doi:10.1016/j.bbrc.2019.06.117.

Muscle fiber-type selective propensity to pathology in the *nmd* mouse model of SMARD1

Eric Villalón[1,2], **Naomi N. Lee**[2], **Jose Marquez**[1], **Christian L. Lorson**[1,2,*]

[1]Bond Life Sciences Center, University of Missouri, Columbia, MO, 65211

[2]Department of Veterinary Pathobiology, College of Veterinary Medicine, University of Missouri, Columbia, MO, 65211

Abstract

Spinal muscular atrophy with respiratory distress type 1 (SMARD1) is an autosomal recessive disease that causes distal limb muscle atrophy, due to motor neuron degeneration. Similar to other motor neuron diseases, SMARD1 shows differential vulnerability to denervation in various muscle groups, which is recapitulated in the *nmd* mouse, a model of SMARD1. In multiple neurodegenerative disease models, transcriptomic analysis has identified differentially expressed genes between vulnerable motor neuron populations, but the mechanism leading to susceptibility is largely unknown. To investigate if denervation vulnerability is linked to intrinsic muscle properties, we analyzed muscle fiber-type composition in muscles from motor units that show different degrees of denervation in *nmd* mice: gastrocnemius, tibialis anterior (TA), and extensor digitorum longus (EDL). Our results revealed that denervation vulnerability correlated with atrophy and loss of MyHC-IIb and MyHC-IIx muscle fiber types. Interestingly, increased vulnerability also correlated with an increased abundance of MyHC-I and MyHC-IIa muscle fibers. These results indicated that MyHC-IIx muscle fibers are the most vulnerable to denervation, followed by MyHC-IIb muscle fibers. Moreover, our data indicate that type MyHC-IIa and MyHC-IIb muscle fibers show resistance to denervation and compensate for the loss of MyHC-IIx and MyHC-IIb muscle fibers in the most vulnerable muscles. Taken together these results provide a basis for the selective vulnerability to denervation of specific muscles in *nmd* mice and identifies new targets for potential therapeutic intervention.

Keywords

Spinal muscular atrophy with respiratory distress; SMARD1; Neurodegeneration; Neuromuscular junction; Disease pathology

*To whom correspondence should be addressed: Christian L. Lorson, Department of Veterinary Pathobiology, Christopher S. Bond Life Sciences Center, 1201 Rollins, Room 471G, University of Missouri, Columbia, MO 65211-7310, USA, Tel: +1 573 884 2219, Fax: +1 573 884 9395, lorsonc@missouri.edu.
C.L.L. is the co-founder and Chief Scientific Officer of Shift Pharmaceuticals.

Introduction

Spinal muscular atrophy with respiratory distress type 1 (SMARD1, OMIM 604320) is a fatal, early-onset, motor neuron disease for which not treatment is available [1,2]. SMARD1 begins during infancy with severe distal limb muscle atrophy that progresses proximally and eventually ends in death due to diaphragmatic paralysis within 2 years of age [1,3-5]. Muscle atrophy is a result of neuromuscular junction (NMJ) denervation caused by selective loss of alpha motor neurons [6,7]. Genetically, SMARD1 is caused by the loss-of-function the immunoglobulin-μ-binding protein 2 (IGHMBP2) gene located in chromosome 11q13.3 [3,8-10]. IGHMBP2 is a ubiquitously expressed protein whose best described function is in translation through interactions with factors including tRNA Tyr, Reptin, Potin, TFIIIC220, and ABT1 [11]. IGHMBP2 is known to contain an RNA/DNA helicase domain, an ATP binding motif, a zinc finger domain, and a nucleic acid binding domain homologous to the UPF1-like superfamily 1 helicases [8,12-14]. Data form human patients has shown that most of the intragenic mutations that lead to motor neuron loss reside within these functional domains (1, 2, 15, 16). Although, IGHMBP2 is ubiquitously expressed, the mechanisms by which loss of function leads to selective loss of alpha motor neurons is not understood (18-20).

The neuromuscular degeneration (*nmd*) mouse is a reliable model for the study of this disease [15-17]. *nmd* mice harbor a mutation within intron 4 of the *Ighmbp2* gene, resulting in a cryptic splice site that leads to aberrant *Ighmbp2* mRNA splicing and a ~75-80% reduction in fully functional Ighmbp2 protein [15,18]. The *nmd* mice develop hind limb muscle weakness by postnatal day (PND) 21 and severe atrophy and paralysis of hind muscles by five weeks of age [15-17]. *nmd* mice develop a significant, 40%, loss of motor neurons prior to onset of overt symptoms, which is followed by a plateau and then progressive motor neuron degeneration until death [7,16]. Early loss of motor neurons as well as loss of large caliber axons in distal peripheral nerves, which correlate with NMJ denervation, are features shared by the *nmd* mouse model and SMARD1 patients [5,7,16,19,20]. Interestingly, *nmd* mice develop dilated cardiomyopathy by final stages of disease leading to death, which is not typically observed in human patients [1,17].

Similar to other motor neuron diseases, SMARD1 is characterized by selective and specific loss of alpha motor neurons [21-26]. Recent systemic analyses of NMJ denervation in various clinically relevant muscles revealed that *nmd* mice develop vulnerability to pathology within specific motor units, suggesting that specific motor neurons are more prone to pathology than others [27]. Interestingly, vulnerability to denervation did not correlate with muscle group anatomical location or specific function [27]. This suggests that there is a different factor that confers vulnerability or protection that is different in each muscle group. Identifying the specific factor that leads to increased vulnerability in different muscles will expand our understanding of SMARD1 disease mechanisms and identify new targets for possible therapeutic intervention.

Skeletal muscle is made up different subtypes of muscle fibers, which are classified according to the myosin heavy chain (MyHC) isoform expression and metabolic activity [Reviewed in 28]. Muscle fibers are classified in four main types: type-I are slow-twitch

oxidative fibers (MyHC-I); type-IIa are fast-twitch oxidative fibers (MyHC-IIa); type-IIb are fast-twitch glycolytic fibers (MyHC-IIb); and type IIx are fast twitch glycolytic fibers (MyHC-IIx) [Reviewed in 28]. Interestingly, muscle fiber sub-types are differentially affected by atrophic factors. For example, sepsis and cancer cachexia lead to atrophy of type II fibers [29], long-term microgravity exposure causes atrophy of type I muscle fibers [30], and inactivity causes atrophy and loss of type-I muscle fibers while increasing type-II muscle fiber abundance [31]. These data indicate that the fiber-type composition of each muscle is an important determinant of vulnerability to pathology in different atrophic conditions. To investigate if SMARD1 selectively affects specific fiber-types, and thus fiber type composition determines the level of vulnerability, we investigated fiber-type composition and atrophy in three differentially vulnerable muscles.

Materials and Methods

Animal procedures

SMARD1 model mice (*nmd*) (B6.BKS- Ighmbp2nmd-2J/J) were purchased commercially (Jackson Laboratories Bar Harbor, ME) and a colony was established. All animal experiments took place in accordance with procedures approved by NIH guidelines and MU Animal Care and Use Committee. SMARD1 animals were genotyped at P1 according to the genotyping procedure in Jax mice resources. Wildtype and *nmd* littermate mice were allowed to age to 8 weeks old.

Immunohistochemistry

For detection of specific individual fiber-types, 8-week-old wildtype and *nmd* mice were anesthetized with 2.5% isoflurane and sacrificed by cervical dislocation. Gastrocnemius, TA, and EDL muscles were dissected and flash frozen in liquid nitrogen. Muscles cross-sections were made using a cryostat and mounted on positively charged microscope slides. Sections were kept at −80 until stained. Slides were blocked with 10% NGS, 1% Nonidet-P40 for 1 hour at 4 °C, then primary antibody solution was added in blocking solution and incubated overnight at 4 °C. Slides were then washed 3X with 1X PBS for 5 min and fixed with 4% PFA for 10 min at 4 °C. Secondary antibodies were added in blocking solution and slides were incubated for 2 hours at room temperature followed by 3X washes with 1X PBS for 5 minutes and then coverslips were mounted. Antibodies:rabbit anti-laminin, 1:400 (Sigma-Aldrich), mouse anti-MyHC-I (1:20), -IIa (1:10), and -IIb (1:5) (clones BA-D5, SC-71, and BFF3; Developmental Studies Hybridoma Bank).

Imaging

Whole section tiling z-stack images were taken using a laser scanning confocal microscope (20x objective; Leica TCS SP8, Leica Microsystems Inc.). Muscle cross section images were analyzed using the freely available Fiji Software (NIH). Laminin staining was used for outlining individual myofibers. The total number of myofibers was counted in each muscle cross-section (1 section per muscle) (n=3 animals per genotype). The total number of individual fiber-types were counted using sections stained with each corresponding type antibody. To count MyHC-IIx fibers, a section stained with all three MyHC antibodies was used and only fibers not stained were counted. Fiber area was measured in the same images

as the fiber counts. Averages for counts and areas were calculated for each genotype and analyzed for statistical significance.

Statistics

Statistical analyses were performed using GraphPad Prism version 6.0 (GraphPad Software Inc.) Muscle fiber counts and fiber area data were analyzed by Student's t-test. N=3 animals per genotype. p value < 0.05 was considered statistically significant.

Results

Specific muscle fiber types were successfully detected by immunofluorescence in all muscles analyzed.

To investigate if denervation vulnerability correlates with muscle fiber-type composition in *nmd* mice, three muscles with different degrees of vulnerability to disease development were isolated from 2-month-old mice. The gastrocnemius muscle, tibialis anterior (TA) and extensor digitorum longus (EDL) present with a range of denervation from high to low, respectively, in *nmd* mice [27]. To detect the various muscle fiber types, isoform-specific antibodies were used to detect the MyHC expression profiles. Slow muscle fibers (MyHC-I) and fast muscle fibers (MyHC-IIa, and MyHC-IIB) were detected by immunohistochemistry of muscles sections from 8-week-old wildtype and *nmd* mice (Fig. 1). Fast muscle fibers expressing MyHC-IIx were identified by the lack of labeling when MyHC-I, MyHC-IIa and MyHC-IIb were used in combination (Fig. 1). Immunohistochemistry showed that all four muscle fiber types were successfully detected in Gastrocnemius, TA, and EDL muscles (Fig. 1A-C, respectively) of *nmd* and wildtype mice.

Increased vulnerability to denervation correlates with loss of MyHC-IIx and MyHC-IIb muscle fibers in *nmd* mice.

To investigate if loss of any muscle fiber type specifically correlated with vulnerability to denervation in *nmd* mice, the total number of each fiber type in each muscle was determined. In the gastrocnemius, most severely denervated muscle, *nmd* muscles displayed a significant 8.9-fold increase in the number of MyHC-I fibers and a 2.8-fold increase in the number of MyHC-IIa fibers compared to wildtype controls (Fig. 2A). MyHC-IIb and MyHC-IIx muscle fibers both showed a significant reduction (~65%) in *nmd* mice compared to wildtype (Fig. 2A). As expected, the total number of muscle fibers in the *nmd* gastrocnemius muscle was significantly reduced by ~60% compared to wildtype. In the TA muscle, no significant changes were observed in MyHC-I and MyHC-IIb muscle fibers in *nmd* compared to wildtype (Fig. 2B). However, the number of MyHC-IIa was significantly increased by 6.3-fold, while MyHC-IIx muscle fibers were significantly reduced by ~97% in *nmd* mice compared to wildtype controls (Fig. 2B). Interestingly, the total number of muscle fibers in TA muscle was not different in *nmd* mice compared to wildtype controls. In the EDL, the least vulnerable muscle analyzed here, the number of MyHC-I muscle fibers were significantly decreased by 75% in *nmd* mice compared to wildtype (Fig. 2C). No difference in the number of MyHC-IIa and MyHC-IIb muscle fibers was found in the EDL muscle while the number MyHC-IIx was significantly lowered by ~ 92% in *nmd* compared to wildtype controls (Fig. 2C). Moreover, the total number of fibers in EDL showed a ~ 10%

decrease (statistically significant) in *nmd* mice compared to wildtype. These data show that type-IIx and type-IIb muscle fibers are lost more prominently and type-IIa and type-I compensate by increasing in abundance.

Fast muscle fibers expressing MyHC-IIb and MyHC-IIx show severe atrophy in vulnerable muscles of *nmd*.

Muscle denervation without re-innervation leads to muscle fiber atrophy and degeneration [32,33]. To investigate fiber-type specific atrophy in differentially vulnerable muscles we measured cross sectional area for each muscle fiber-type gastrocnemius, TA and EDL muscles. Measurements from the gastrocnemius muscle showed a slight, non-statistically significant, increase in MyHC-I fiber area in *nmd* mice compared to wildtype (Fig. 3A). MyHC-IIa, MyHC-IIb, and MyHC-IIx fiber cross sectional areas were all significantly decreased by ~ 25%, ~75%, and ~92%, respectively, in *nmd* mice compared to wildtype (Fig. 3A). Measurements form the TA muscle showed no difference in MyHC-I and MyHC-IIa fiber area between *nmd* and wildtype controls. However, both MyHC-IIb and MyHC-IIx were significantly decreased by ~ 46%, and ~70%, respectively, in *nmd* compared to wildtype controls (Fig. 3B). EDL muscle showed a significant decrease of ~42% in MyHC-I fiber area while no difference in MyHC-IIa area was observed between *nmd* and wildtype controls (Fig. 3C). MyHC-IIb and MyHC-IIx fiber area was significantly decreased by ~20% and ~71%, respectively, in *nmd* mice compared to controls (Fig. 3C). These data demonstrate that Type IIx and IIb fibers are the most affected while type-IIa are the most resistant to atrophy in *nmd* mice.

Discussion

In this study we sought to gain further understanding of the intrinsic factors that play a role in conferring selective vulnerability in different muscles affected with SMARD1. Analysis of muscle fiber-type specific changes in three muscles with varying degrees of vulnerability revealed that fast-twitch glycolytic fibers (type IIx and type IIb) are the most severely affected in SMARD1. Moreover, the magnitude of fiber loss and the degree of fiber atrophy correlated with the degree of vulnerability. This suggests that the relative composition of type-IIb and IIx fibers impacts the degree of vulnerability in each muscle group. Moreover, our analyses revealed an increase in the number of slow-twitch oxidative (type-I) and fast-twitch oxidative (type-IIa) fibers that correlated with increased vulnerability suggesting that oxidative fibers are the most resistant to pathology. Taken together these results indicate that numbers of fast-twitch glycolytic fibers determines the degree of vulnerability, while increased levels of oxidative fibers determines the relative resistance to degeneration in different muscles in *nmd* mice. These results shed new light into our understanding of the mechanisms that cause to selective vulnerability to pathology in different muscles in SMARD1 [27].

Motor neurons are classified as slow, fast-resistant, and fast-fatigable depending on Depending on their electrical firing rate, activation threshold and refractory time [34,35]. This classification mirrors the function of the target muscle fiber as motor neurons determine the fiber type of the myofibers they innervate [36]. Motor neuron loss is the primary cause of

muscle atrophy in SMARD1 [6,7,37], However, it is not clear which type of motor neurons are the most susceptible to degeneration. Our data here shows that fast glycolytic muscle fibers are the most severely affected in SMARD1, which suggests that fast-fatigable motor neurons are also the most susceptible to degeneration. Moreover, given that oxidative fibers appear to be resistant to degeneration suggests that slow, and slow-resistant motor neurons are also the most resistant to degeneration in SMARD1. These results expand our understanding of pathology development and identify new and specific cell-types that are selectively and most prominently affected in SMARD1. Moving forward, this new information will allow the comparison of genetic differences between fast-fatigable and slow motor units for identification of genetic factors responsible for providing resistance to degeneration. Finally, this work provides sensitive targets for the development and exploration of new therapeutics for the treatment of SMARD1.

Acknowledgements

We would like to thank members of the Lorson lab who contributed to the early stages of this project and to animal colony maintenance. This work was supported by the National Institute of Health (R21NS109762) to CLL and JM is supported by NIH PREP (R25GM064120).

References

[1]. Eckart M, Guenther UP, Idkowiak J, Varon R, Grolle B, Boffi P, Van Maldergem L, Hubner C, Schuelke M, von Au K, The natural course of infantile spinal muscular atrophy with respiratory distress type 1 (SMARD1), Pediatrics 129 (2012) e148–156. 10.1542/peds.2011-0544. [PubMed: 22157136]

[2]. Grohmann K, Schuelke M, Diers A, Hoffmann K, Lucke B, Adams C, Bertini E, Leonhardt-Horti H, Muntoni F, Ouvrier R, Pfeufer A, Rossi R, Van Maldergem L, Wilmshurst JM, Wienker TF, Sendtner M, Rudnik-Schoneborn S, Zerres K, Hubner C, Mutations in the gene encoding immunoglobulin mu-binding protein 2 cause spinal muscular atrophy with respiratory distress type 1, Nat Genet 29 (2001) 75–77. 10.1038/ng703. [PubMed: 11528396]

[3]. Grohmann K, Wienker TF, Saar K, Rudnik-Schoneborn S, Stoltenburg-Didinger G, Rossi R, Novelli G, Nurnberg G, Pfeufer A, Wirth B, Reis A, Zerres K, Hubner C, Diaphragmatic spinal muscular atrophy with respiratory distress is heterogeneous, and one form Is linked to chromosome 11q13-q21, American journal of human genetics 65 (1999) 1459–1462. 10.1086/302636. [PubMed: 10521314]

[4]. Porro F, Rinchetti P, Magri F, Riboldi G, Nizzardo M, Simone C, Zanetta C, Faravelli I, Corti S, The wide spectrum of clinical phenotypes of spinal muscular atrophy with respiratory distress type 1: a systematic review, J Neurol Sci 346 (2014) 35–42. 10.1016/j.jns.2014.09.010. [PubMed: 25248952]

[5]. Grohmann K, Varon R, Stolz P, Schuelke M, Janetzki C, Bertini E, Bushby K, Muntoni F, Ouvrier R, Van Maldergem L, Goemans NM, Lochmuller H, Eichholz S, Adams C, Bosch F, Grattan-Smith P, Navarro C, Neitzel H, Polster T, Topaloglu H, Steglich C, Guenther UP, Zerres K, Rudnik-Schoneborn S, Hubner C, Infantile spinal muscular atrophy with respiratory distress type 1 (SMARD1), Ann Neurol 54 (2003) 719–724. 10.1002/ana.10755. [PubMed: 14681881]

[6]. Wong VC, Chung BH, Li S, Goh W, Lee SL, Mutation of gene in spinal muscular atrophy respiratory distress type I, Pediatr Neurol 34 (2006) 474–477. 10.1016/j.pediatrneurol.2005.10.022. [PubMed: 16765827]

[7]. Krieger F, Elflein N, Ruiz R, Guerra J, Serrano AL, Asan E, Tabares L, Jablonka S, Fast motor axon loss in SMARD1 does not correspond to morphological and functional alterations of the NMJ, Neurobiol Dis 54(2013) 169–182. 10.1016/j.nbd.2012.12.010. [PubMed: 23295857]

[8]. Guenther UP, Handoko L, Laggerbauer B, Jablonka S, Chari A, Alzheimer M, Ohmer J, Plottner O, Gehring N, Sickmann A, von Au K, Schuelke M, Fischer U, IGHMBP2 is a ribosome-

associated helicase inactive in the neuromuscular disorder distal SMA type 1 (DSMA1), Hum Mol Genet 18 (2009)1288–1300.10.1093/hmg/ddp028. [PubMed: 19158098]

[9]. Viollet L, Barois A, Rebeiz JG, Rifai Z, Burlet P, Zarhrate M, Vial E, Dessainte M, Estournet B, Kleinknecht B, Pearn J, Adams RD, Urtizberea JA, Cros DP, Bushby K, Munnich A, Lefebvre S, Mapping of autosomal recessive chronic distal spinal muscular atrophy to chromosome 11q13, Ann Neurol 51 (2002) 585–592.10.1002/ana.10182. [PubMed: 12112104]

[10]. Fukita Y, Mizuta TR, Shirozu M, Ozawa K, Shimizu A, Honjo T, The human S mu bp-2, a DNA-binding protein specific to the single-stranded guanine-rich sequence related to the immunoglobulin mu chain switch region, J Biol Chem 268 (1993) 17463–17470. [PubMed: 8349627]

[11]. de Planell-Saguer M, Schroeder DG, Rodicio MC, Cox GA, Mourelatos Z, Biochemical and genetic evidence for a role of IGHMBP2 in the translational machinery, Hum Mol Genet 18 (2009) 2115–2126. 10.1093/hmg/ddp134. [PubMed: 19299493]

[12]. Jankowsky A, Guenther UP, Jankowsky E, The RNA helicase database, Nucleic Acids Res 39 (2011) D338–341. 10.1093/nar/gkq1002. [PubMed: 21112871]

[13]. Chen NN, Kerr D, Chang CF, Honjo T, Khalili K, Evidence for regulation of transcription and replication of the human neurotropic virus JCV genome by the human S(mu)bp-2 protein in glial cells, Gene 185 (1997) 55–62. [PubMed: 9034313]

[14]. Miao M, Chan SL, Fletcher GL, Hew CL, The rat ortholog of the presumptive flounder antifreeze enhancer-binding protein is a helicase domain-containing protein, Eur J Biochem 267 (2000) 7237–7246. [PubMed: 11106437]

[15]. Cook SA, Johnson KR, Bronson RT, Davisson MT, Neuromuscular degeneration (nmd): a mutation on mouse chromosome 19 that causes motor neuron degeneration, Mamm Genome 6 (1995) 187–191. [PubMed: 7749225]

[16]. Grohmann K, Rossoll W, Kobsar I, Holtmann B, Jablonka S, Wessig C, Stoltenburg-Didinger G, Fischer U, Hubner C, Martini R, Sendtner M, Characterization of Ighmbp2 in motor neurons and implications for the pathomechanism in a mouse model of human spinal muscular atrophy with respiratory distress type 1 (SMARD1), Hum Mol Genet 13 (2004) 2031–2042. 10.1093/hmg/ddh222. [PubMed: 15269181]

[17]. Maddatu TP, Garvey SM, Schroeder DG, Hampton TG, Cox GA, Transgenic rescue of neurogenic atrophy in the nmd mouse reveals a role for Ighmbp2 in dilated cardiomyopathy, Hum Mol Genet 13 (2004) 1105–1115. 10.1093/hmg/ddh129. [PubMed: 15069027]

[18]. Cox GA, Mahaffey CL, Frankel WN, Identification of the mouse neuromuscular degeneration gene and mapping of a second site suppressor allele, Neuron 21 (1998) 1327–1337. [PubMed: 9883726]

[19]. Diers A, Kaczinski M, Grohmann K, Hubner C, Stoltenburg-Didinger G, The ultrastructure of peripheral nerve, motor end-plate and skeletal muscle in patients suffering from spinal muscular atrophy with respiratory distress type 1 (SMARD1), Acta Neuropathol 110 (2005) 289–297. 10.1007/s00401-005-1056-y. [PubMed: 16025284]

[20]. Luan X, Huang X, Liu X, Zhou H, Chen S, Cao L, Infantile spinal muscular atrophy with respiratory distress type I presenting without respiratory involvement: Novel mutations and review of the literature, Brain & development 38 (2016) 685–689. 10.1016/j.braindev.2016.02.001. [PubMed: 26922252]

[21]. Nijssen J, Comley LH, Hedlund E, Motor neuron vulnerability and resistance in amyotrophic lateral sclerosis, Acta Neuropathol 133 (2017) 863–885. 10.1007/s00401-017-1708-8. [PubMed: 28409282]

[22]. Comley LH, Nijssen J, Frost-Nylen J, Hedlund E, Cross-disease comparison of amyotrophic lateral sclerosis and spinal muscular atrophy reveals conservation of selective vulnerability but differential neuromuscular junction pathology, J Comp Neurol 524 (2016) 1424–1442. 10.1002/cne.23917. [PubMed: 26502195]

[23]. Grunseich C, Rinaldi C, Fischbeck KH, Spinal and bulbar muscular atrophy: pathogenesis and clinical management, Oral Dis 20 (2014) 6–9. 10.1111/odi.12121. [PubMed: 23656576]

[24]. Murray LM, Lee S, Baumer D, Parson SH, Talbot K, Gillingwater TH, Pre-symptomatic development of lower motor neuron connectivity in a mouse model of severe spinal muscular atrophy, Hum Mol Genet 19(2010) 420–433.10.1093/hmg/ddp506. [PubMed: 19884170]

[25]. Piepers S, van der Pol WL, Brugman F, Wokke JH, van den Berg LH, Natural history of SMA IIIb: muscle strength decreases in a predictable sequence and magnitude, Neurology 72(2009)2057–2058; author reply 2058. 10.1212/01.wnl.0000349698.94744.1e. [PubMed: 19506238]

[26]. Murray LM, Comley LH, Thomson D, Parkinson N, Talbot K, Gillingwater TH, Selective vulnerability of motor neurons and dissociation of pre- and post-synaptic pathology at the neuromuscular junction in mouse models of spinal muscular atrophy, Hum Mol Genet 17 (2008) 949–962. 10.1093/hmg/ddm367. [PubMed: 18065780]

[27]. Villalon E, Shababi M, Kline R, Lorson ZC, Florea KM, Lorson CL, Selective vulnerability in neuronal populations in nmd/SMARD1 mice, Hum Mol Genet 27 (2018) 679–690. 10.1093/hmg/ddx434. [PubMed: 29272405]

[28]. Schiaffino S, Reggiani C, Fiber types in mammalian skeletal muscles, Physiol Rev 91 (2011) 1447–1531. 10.1152/physrev.00031.2010. [PubMed: 22013216]

[29]. Reed SA, Sandesara PB, Senf SM, Judge AR, Inhibition of FoxO transcriptional activity prevents muscle fiber atrophy during cachexia and induces hypertrophy, Faseb J 26 (2012) 987–1000. 10.1096/fj.11-189977. [PubMed: 22102632]

[30]. Sandona D, Desaphy JF, Camerino GM, Bianchini E, Ciciliot S, Danieli-Betto D, Dobrowolny G, Furlan S, Germinario E, Goto K, Gutsmann M, Kawano F, Nakai N, Ohira T, Ohno Y, Picard A, Salanova M, Schiffl G, Blottner D, Musaro A, Ohira Y, Betto R, Conte D, Schiaffino S, Adaptation of mouse skeletal muscle to long-term microgravity in the MDS mission, PLoS One 7 (2012) e33232 10.1371/journal.pone.0033232. [PubMed: 22470446]

[31]. Grossman EJ, Roy RR, Talmadge RJ, Zhong H, Edgerton VR, Effects of inactivity on myosin heavy chain composition and size of rat soleus fibers, Muscle Nerve 21 (1998) 375–389. [PubMed: 9486867]

[32]. Bongers KS, Fox DK, Ebert SM, Kunkel SD, Dyle MC, Bullard SA, Dierdorff JM, Adams CM, Skeletal muscle denervation causes skeletal muscle atrophy through a pathway that involves both Gadd45a and HDAC4, Am J Physiol Endocrinol Metab 305 (2013) E907–915. 10.1152/ajpendo.00380.2013. [PubMed: 23941879]

[33]. Rowan SL, Rygiel K, Purves-Smith FM, Solbak NM, Turnbull DM, Hepple RT, Denervation causes fiber atrophy and myosin heavy chain co-expression in senescent skeletal muscle, PLoS One 7 (2012) e29082 10.1371/journal.pone.0029082. [PubMed: 22235261]

[34]. Garnett RA, O'Donovan MJ, Stephens JA, Taylor A, Motor unit organization of human medial gastrocnemius, J Physiol 287(1979)33–43. 10.1113/jphysiol.1979.sp012643. [PubMed: 430414]

[35]. Hamm TM, Nemeth PM, Solanki L, Gordon DA, Reinking RM, Stuart DG, Association between biochemical and physiological properties in single motor units, Muscle Nerve 11 (1988) 245–254. 10.1002/mus.880110309. [PubMed: 3352659]

[36]. Kanning KC, Kaplan A, Henderson CE, Motor neuron diversity in development and disease, Annual review of neuroscience 33(2010)409–440. 10.1146/annurev.neuro.051508.135722.

[37]. Shababi M, Feng Z, Villalon E, Sibigtroth CM, Osman EY, Miller MR, Williams-Simon PA, Lombardi A, Sass TH, Atkinson AK, Garcia ML, Ko CP, Lorson CL, Rescue of a Mouse Model of Spinal Muscular Atrophy With Respiratory Distress Type 1 by AAV9-IGHMBP2 Is Dose Dependent, Molecular therapy : the journal of the American Society of Gene Therapy 24 (2016) 855–866. 10.1038/mt.2016.33. [PubMed: 26860981]

Denervation vulnerability in the nmd mouse correlates with fiber type loss.

Muscle properties may dictate intrinsic susceptibility to motor unit degeneration.

Spatial and temporal development does not necessarily dictate motor unit vulnerability.

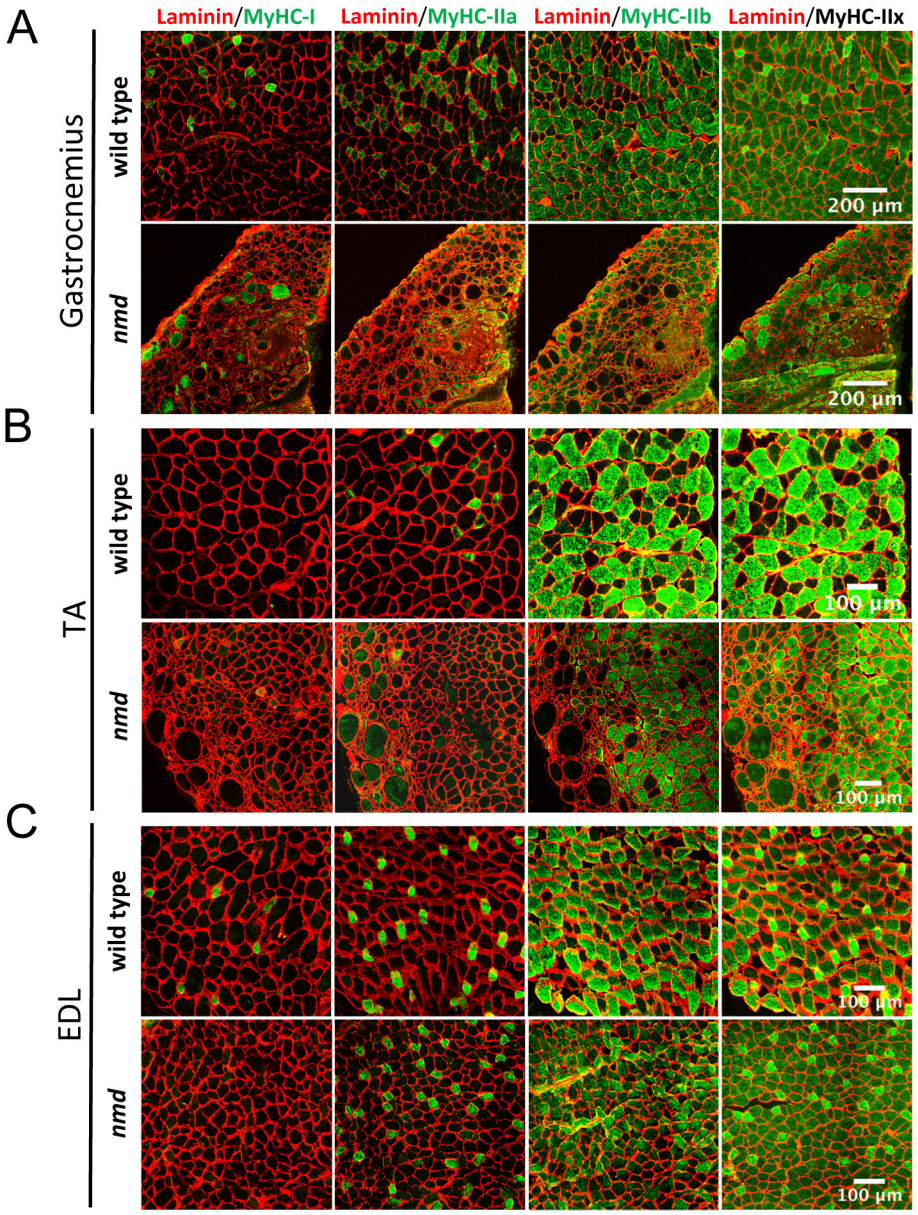

Figure 1. Detection of muscle fiber subtype in gastrocnemius, TA, and EDL muscles.

8-week-old gastrocnemius, TA, and EDL muscle sections were immunostained to label the muscle fiber outline (laminin), type I (MyHC-I), type IIa (MyHC-IIa), type IIb (MyHC-IIb) fibers. Type IIx fibers were identified by the lack of staining when MyHC -I, -IIa, -IIb were combined on the same section. **A-C)** Representative images of the gastrocnemius (**A**) (scale bar = 200 μm), TA (**B**) (scale bar = 100 μm), and EDL (**C**) (scale bar = 100 μm) cross sections stained to identify individual muscle fibers and their outline in wildtype and *nmd* muscles. Maximum projection confocal images taken at 20x. n = 3 animals per genotype.

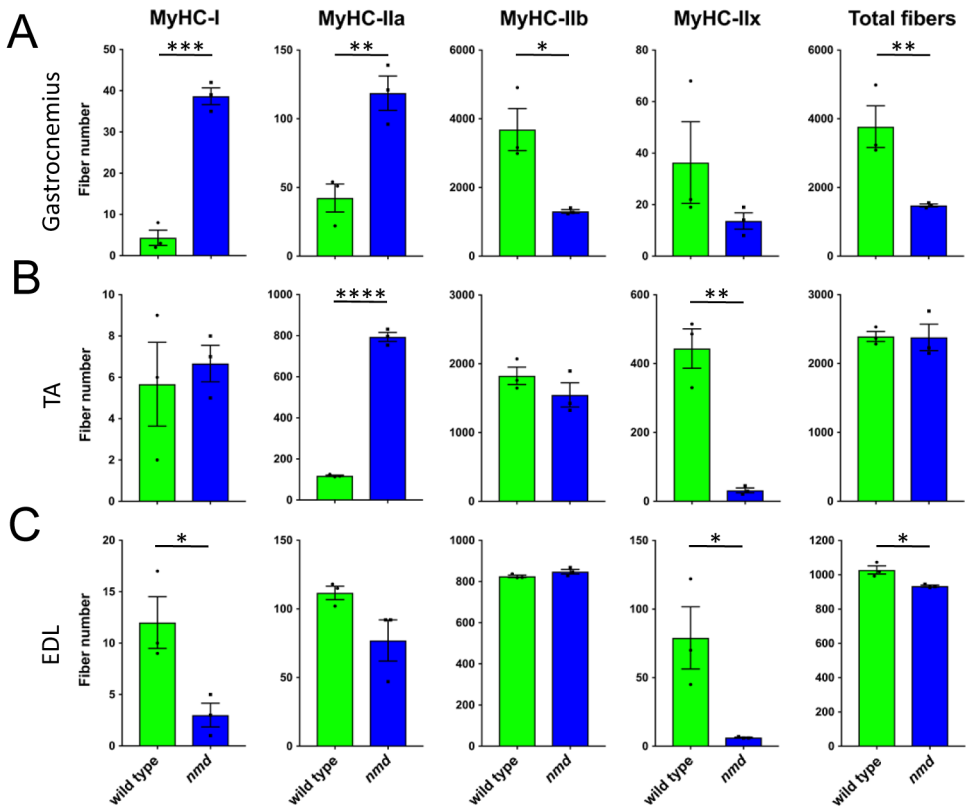

Figure 2. Type-IIx and type IIb fibers numbers are the most severely decreased in muscles with higher vulnerability in *nmd* mice.

Quantification of muscle fiber numbers for each individual fiber type and for total number of fibers in muscles of 8-week-old *nmd* and wildtype controls. **A)** Gastrocnemius muscle fiber counts showed a significant increase in type I (MyHC-I) ($p = 0.0002$) and type IIa (MyHC-IIa) ($p = 0.0091$), while type IIb (MyHC-IIb) ($p = 0.0179$) and type IIx (MyHC-IIx) (Not significant, $p = 0.2337$) were severely decreased in *nmd* mice compared to wildtype. As expected the total number of fibers was significantly decreased in *nmd* mice compared to wildtype. **B)** TA muscle had a significant increase ($p < 0.0001$) in type I fiber number and a significant decrease ($p = 0.0021$) in type IIb fiber number in *nmd* mice compared to wildtype. **C)** EDL muscle had a significant decrease in type I ($p = 0.0314$), type IIx ($p = 0.0326$), and total ($p = 0.0180$) fiber numbers in nmd compared to wildtype. Data were analyzed by a Student's t-test. Data expressed as mean ± SEM. $n = 3$ animals per genotype.

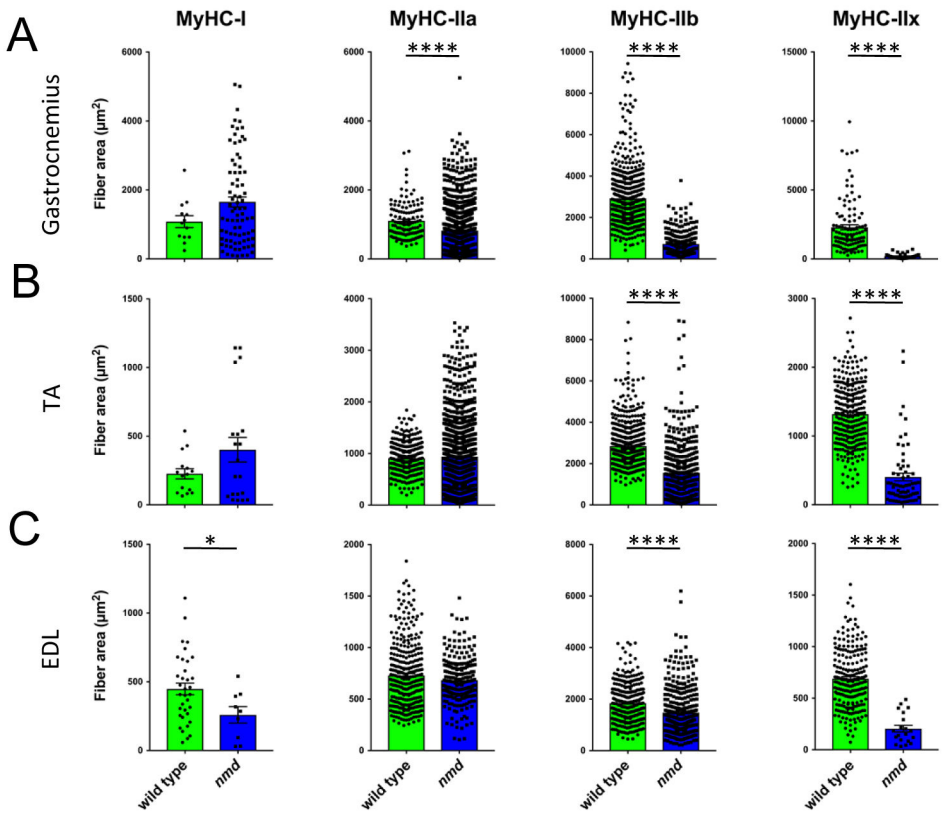

Figure 3. Type IIx and type IIb fibers are more severely atrophied in muscles with increased vulnerability in *nmd* mice.

Quantification of muscle fiber area for each fiber type in muscles of 8-week-old *nmd* and wildtype mice. **A)** Gastrocnemius muscle showed a significant reduction in fiber area of type IIa ($p < 0.00010$, type IIb ($p < 0.0001$), and type IIx ($p < 0.0001$) in *nmd* compared to wildtype mice. **B)** TA muscle showed a significant decrease in type IIb ($p < 0.0001$) and type IIx ($p < 0.0001$) fiber area in *nmd* compared to wildtype mice. **C)** Similarly, the EDL muscle showed a significant decrease in type IIb ($p < 0.0001$) and type IIx ($p < 0.0001$) muscle fiber area in *nmd* compared to wildtype mice. Data were analyzed by a Student's t-test. Data expressed as mean ± SEM. n = 3 animals per genotype.